JACS
JOURNAL OF THE AMERICAN CHEMICAL SOCIETY
pubs.acs.org/JACS
Communication

Selective Anion Binding Drives the Formation of $Ag^{I}_{8}L_6$ and $Ag^{I}_{12}L_6$ Six-Stranded Helicates

Charlie T. McTernan, Tanya K. Ronson, and Jonathan R. Nitschke*

Cite This: J. Am. Chem. Soc. 2021, 143, 664–670
Read Online
ACCESS | Metrics & More | Article Recommendations | Supporting Information

ABSTRACT: Here we describe the formation of an unexpected and unique family of hollow six-stranded helicates. The formation of these structures depends on the coordinative flexibility of silver and the 2-formyl-1,8-napthyridine subcomponent. Crystal structures show that these assemblies are held together by Ag_4I, Ag_4Br, or $Ag_6(SO_4)_2$ clusters, where the templating anion plays an integral structure-defining role. Prior to the addition of the anionic template, no six-stranded helicate was observed to form, with the system instead consisting of a dynamic mixture of triple helicate and tetrahedron. Six-stranded helicate formation was highly sensitive to the structure of the ligand, with minor modifications inhibiting its formation. This work provides an unusual example of mutual stabilization between metal clusters and a self-assembled metal−organic cage. The selective preparation of this anisotropic host demonstrates new modes of guiding selective self-assembly using silver(I), whose many stable coordination geometries render design difficult.

Self-assembly can produce complex metal−organic architectures from simple starting materials.[1−5] Such structures have been the subject of intense recent exploration, with applications spanning guest binding, stabilization of reactive species, biomolecular interactions, and chemical purification.[6−9] These applications often depend on binding a target in the pseudospherical cavity of a metal−organic cage. These isotropic cavities can bind roughly spherical guests or guest agglomerates[10−13] but are ill-adapted to bind asymmetric and anisotropic guests. The introduction of flexible organic ligands[14−16] or metal coordination spheres[17−20] has led to the formation of new metal−organic cages, with nonspherical internal cavities, partially alleviating these limitations.[21−25] Silver(I), in combination with dipyridyl peptidic linkers, has recently been shown to generate a wealth of complex knotted architectures via self-assembly.[26−28] The strategy of incorporating a guest of interest into the architecture formed, as a template[29−31] or other structural element,[32,33] can enhance selectivity and sensitivity in guest binding.[34−36] Furthermore, if the guest is anionic,[37−39] the diverse coordination chemistry of anions can be used to effect the selective recognition[40−42] of targeted anions.[43]

We hypothesized that the flexible coordination sphere of silver(I) ions,[44−49] in combination with organic ligands that assemble in situ around these metal-ion templates, would provide access to new structure types that bind anions as structural elements. Zhao and co-workers have previously shown that nitrogen containing macrocycles can stabilize atomically precise silver clusters with defined geometries, supporting this hypothesis.[50,51]

Here we describe the formation of a family of complex six-stranded silver helicates upon the addition of three anions: iodide, bromide, and sulfate. This family comprises two novel structure types, with sulfate generating a structure distinct from those templated by halides. Key structural elements within these architectures are unique silver(I)-anion clusters,[50,51] whose geometries are molded by the central anions, which in turn are held in an unusual, polarized, environment.

Building on the discovery that silver(I) assembles with 2-formyl-1,8-naphthyridine (**1**),[52] a tritopic subcomponent, and anionic templates to form a trigonal prism with disilver vertices,[17] we investigated the use of linear ditopic anilines in place of triangular ones. Initial experiments, involving the mixture of benzidine (**2**) together with **1**, various silver salts, and prospective guests in acetonitrile (Figure 1a), gave in all cases an intractable gel (SI Section 8).

Reasoning that increasing steric hindrance and widening the torsion angle between the phenylene groups of the dianiline could lead to a different outcome,[53] we explored the self-assembly of 2,2′-dimethyl-[1,1′-biphenyl]-4,4′-diamine (**3**) with **1** in acetonitrile, and observed the formation of discrete species with various silver(I) salts (Figure 1b). With silver perchlorate, we observed a 1:1 ratio of integrals between two species (Figure 1c). Diffusion ordered spectroscopy (DOSY) NMR revealed that one had a significantly larger diffusion coefficient (Figure 1c). Mass spectrometry indicated that the smaller species had Ag_4L_3 composition, with the larger species corresponding to Ag_8L_6 (Figures S72 and S75). Approximately 400 attempts to grow crystals of these species failed.

The observation of well-defined bands of peaks in the DOSY spectrum is consistent with the formation of discrete species, as opposed to poorly defined oligomers in solution.[54,55] We

Received: November 13, 2020
Published: December 31, 2020

https://dx.doi.org/10.1021/jacs.0c11905
J. Am. Chem. Soc. 2021, 143, 664−670

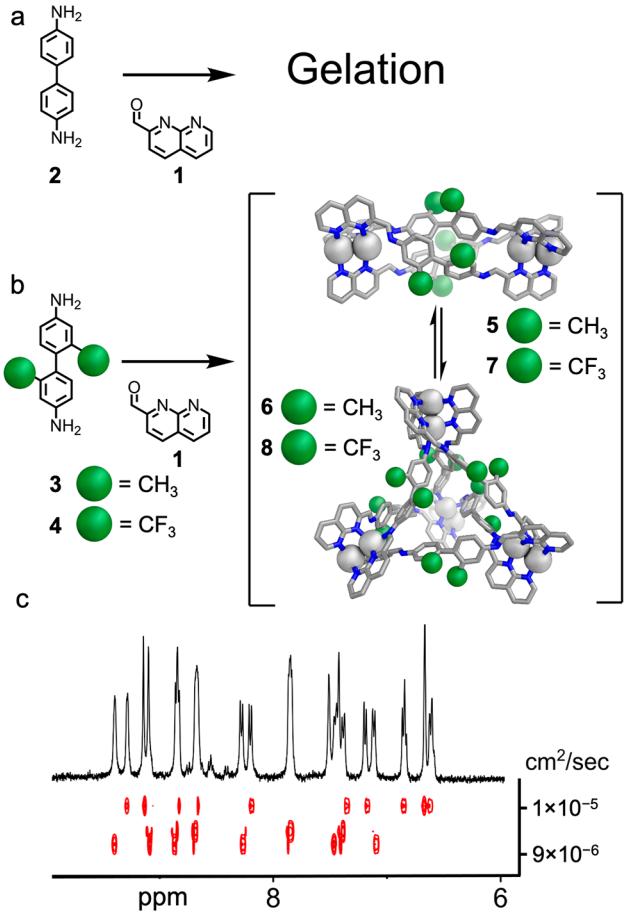

Figure 1. Self-assembly of Ag_4L_3 and Ag_8L_6 architectures. Conditions: (a) $AgNTf_2$ (2 equiv), **2** (1 equiv), **1** (2 equiv), d_3-MeCN, 5 min; (b) $AgNTf_2$ (2 equiv), **3** or **4** (1 equiv), **1** (2 equiv), d_3-MeCN, 5 min. Structures of **5** and **6** are MM3-optimized models. (c) DOSY NMR of **5** and **6**.

modeled potential structures for the Ag_8L_6 architecture and found that a tetrahedral geometry was preferred by 300−400 kcal mol^{-1} (SI Section 9).[56] Although we cannot definitively assign the product structures without crystallographic data, we infer that the two species are likely to be Ag_4L_3 helicate **5** and Ag_8L_6 tetrahedron **6**, consistent with previously reported systems,[57] our modeling studies, and the solution data (SI Section 4.4). Investigations of host−guest behavior showed binding to a range of anionic and organic guests, with some altering the **5**:**6** equilibrium (SI Section 7).[58,59] When dianiline **4** was used in place of **3** we observed similar results (Figure 1b and SI Section 10).

Having extensively screened potential guest species, we next turned to the addition of halides to these silver(I) based assemblies. We had initially avoided the use of halides, anticipating precipitation of silver halide species (the solubility product of AgI is $10^{-14.5}$ in acetonitrile).[60] However, upon addition of TBA iodide, a new species, **9**, immediately formed and, to our surprise, no precipitate was observed.

Characteristic ^{1}H NMR signals were observed for **9** at 6 ppm, ca. 1 ppm upfield of any signals of **5** or **6** (Figure 1c). Furthermore, a twofold desymmetrization was observed, with two ^{1}H NMR signals observed for each proton environment in free ligand (Figure S1). DOSY spectroscopy gave results consistent with the formation of a single species (Figure S8). Mass spectrometry confirmed that a $Ag_8L_6I_2$ architecture had been formed (Figures S69 and S77).[61]

The X-ray crystal structure of **9** revealed its highly unusual six-stranded helicate structure (Figure 3a,b), which is capped at each end by a Ag_4I cluster consisting of a Ag_3 triangle capped by an apical Ag on the outside and iodide on the inside (Figure 3e). The six ligand strands bridge two such Ag_4I clusters, grouped into three pairs of ligands that show aromatic stacking interactions between naphthyridine moieties, with distances of 3.1−3.7 Å between stacked rings.

Atypical coordination environments for the Ag centers were observed in **9**. One arm of each ligand coordinates via all three available nitrogen donors, and the other via only a single inner naphthyridine nitrogen. This differentiation leads to the twofold desymmetrization seen in the ^{1}H NMR spectrum

The presence of 12 uncoordinated nitrogen donors within **9** violates the principle of maximal coordinative saturation, which has often, and successfully, been used to predict the product of metal−organic self-assembly processes.[62] The absence of coordinative stabilization may be a consequence of the nonchelating coordination vectors of **1**, which precluded the formation of simple structures. The lack of coordinative saturation is compensated for by the extensive aromatic stacking seen in the crystal structure of **9**.[63]

Silver−silver separations were 2.96−3.00 Å between silver atoms bridged by a single naphthyridine moiety, greater than those observed in simpler mononuclear naphthyridine-bridged silver complexes.[63] The iodide ion coordinated to all four Ag ions in the cluster, with Ag−I separations of 2.79−2.88 Å, consistent with previous reports of Ag_4I clusters.[50,51]

Having determined the structure of **9**, we investigated whether alternative anions might lead to the generation of further examples of this new structure type. Addition of tetramethylammonium sulfate to a mixture of **1**, **3**, and silver triflimide brought about conversion to an alternate species, **10**, as the uniquely observed product (Figure 2). This product again showed twofold desymmetrization in the ^{1}H NMR (Figure S9) and a single species by DOSY NMR (Figure S14). We initially anticipated that a structure analogous to **9** would be formed, with $Ag_8L_6(SO_4)_2$ stoichiometry, based upon similarities between ^{1}H NMR spectra (Figure S9). However, mass spectrometry indicated that instead a $Ag_{12}L_6(SO_4)_4$ species formed (Figures S70 and S78). Six-stranded helicate formation was confirmed by single-crystal X-ray diffraction (Figure 3c,d). The organic portion of the structure was similar to **9**, yet the silver clusters at the ends of both assemblies are dramatically different. Instead of the Ag_4I clusters of **9**, the vertices of **10** consist of $Ag_6(SO_4)_2$ clusters composed of inner and outer Ag_3 triangles. The externally facing sulfate coordinates to the outer triangle of silver ions via a single, triply coordinated, oxygen atom.[64] The coordination of this sulfate is reinforced by nonclassical hydrogen bonding from three naphthyridine CH groups (CH···O distances 2.40−2.43 Å), stabilizing the assembly (Figure 3f).[65] Each silver ion of this outer triangle is also coordinated by the internal sulfate via a single, triply coordinated oxygen. The interior sulfate additionally coordinates to the internal, more widely spaced, triangle of silver ions. The two Ag triangles form pairs of silver ions in close proximity, with each bridged by two naphthyridine moieties. The sulfur atoms of the internal anions are 11.58 Å apart, farther than the iodide anions in **9** (10.47 Å), and show nonclassical hydrogen bonds (CH···O distances 2.58−2.69 Å) to internally facing CH groups (Figure

https://dx.doi.org/10.1021/jacs.0c11905
J. Am. Chem. Soc. 2021, 143, 664−670

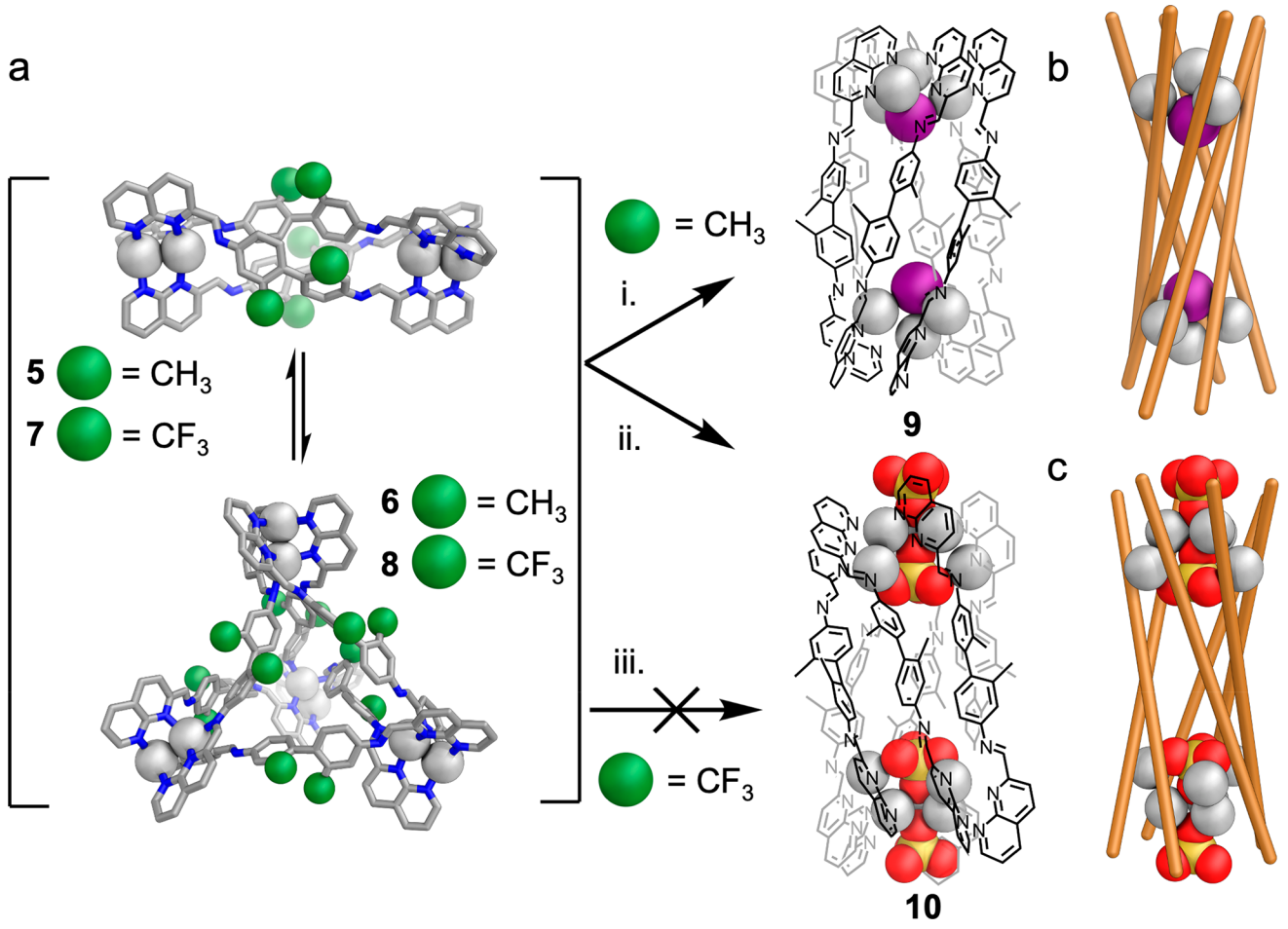

Figure 2. (a) Synthesis of six-stranded helicates **9** and **10**, formed only during self-assembly from dianiline **3**. (i) Tetrabutylammonium iodide (0.34 equiv), 5 min; (ii) tetramethylammonium sulfate (1.0 equiv), 6 h. Structures of **5** and **6** are MM3 optimized models, and those of **9** and **10** are based on crystallographic data (vide infra). Simplified representation of six-stranded helicate (b) **9** and (c) **10**.

3g). Ligand coordination again shows pairwise alternation, here between three and two coordinating nitrogen atoms per ligand arm. The uncoordinated donor atoms were again imine nitrogens

We next investigated whether other anions could template structures similar to **9** and **10**. Among the 38 anions tested (SI Sections 6.7 and 6.8), only bromide proved able to efficiently template a six-stranded helicate (**11**). The ^{1}H NMR spectrum of **11** again exhibited a twofold desymmetrization, and a single species was observed by DOSY spectroscopy, with a hydrodynamic radius of 11.9 Å, similar to the cases of **9** and **10** (Figures S8, S15, and S22). Attempts to grow crystals suitable for X-ray diffraction proved unsuccessful. However, we inferred the $Ag_8L_6Br_2$ structure of **11** to be an analogue of **9** by comparing the ^{1}H NMR, COSY, and HSQC spectra of **9**–**11**. The spectra of **9** and **11** were clearly similar, whereas that of **10** was notably different (Figure 4a and SI Section 5).

We then probed further the selectivity of the assembly process. Silver tetrafluoroborate, hexafluorophosphate, perchlorate, and triflate all furnished six-stranded helicates adopting the framework of **9** when combined with **1**, **3**, and potassium iodide (Figures S38 and S39). Titration of TBA bromide into a mixture of **5** and **6** revealed no intermediate species (i.e., from binding a single bromide). Instead, formation of **11** (containing two bromide anions) was seen immediately, in the continued presence of **5** and **6** (Figures S42 and S46), suggesting that the six-stranded helicate assembled cooperatively (SI Sections 6.3 and 6.6). Using **2** or **4** in place of **3** led to immediate gelation (for **2**) or shifts in the equilibrium of **7** and **8** (for **4**, Figures S55 and S68).

These results highlight the extent to which the subcomponent self-assembly of metal–organic architectures may depend critically upon subtle variations in subcomponent structure. The lack of methyl groups on **2** favored polymerization over the assembly of discrete structures. The subtle steric and electronic differences between the methyl groups of **3** and the trifluoromethyl groups of **4** disfavored, in the latter case, the formation of six-stranded helicates analogous to **9**–**11**. We hypothesize this sensitivity to be due to the slightly weaker ligand field in the case of ligands incorporating **4**, which disfavors structures that incorporate the more highly cationic silver clusters incorporated into the new structure types **9**–**11**.

This work describes the development of a system of novel six-stranded helicates, which assemble around atomically precise silver clusters. Specific anionic templates, in turn, serve to shape these clusters, such that the identity of the anion dictates the architecture observed. The ability of 2-formyl-1,8-napthyridine to bridge silver ions enables these complex structures to form from simple subcomponents. These new assemblies are sensitive to the precise nature of the ligand chosen and are selective for the templates employed, with potential applications in sensing specific analytes.

https://dx.doi.org/10.1021/jacs.0c11905
J. Am. Chem. Soc. 2021, 143, 664–670

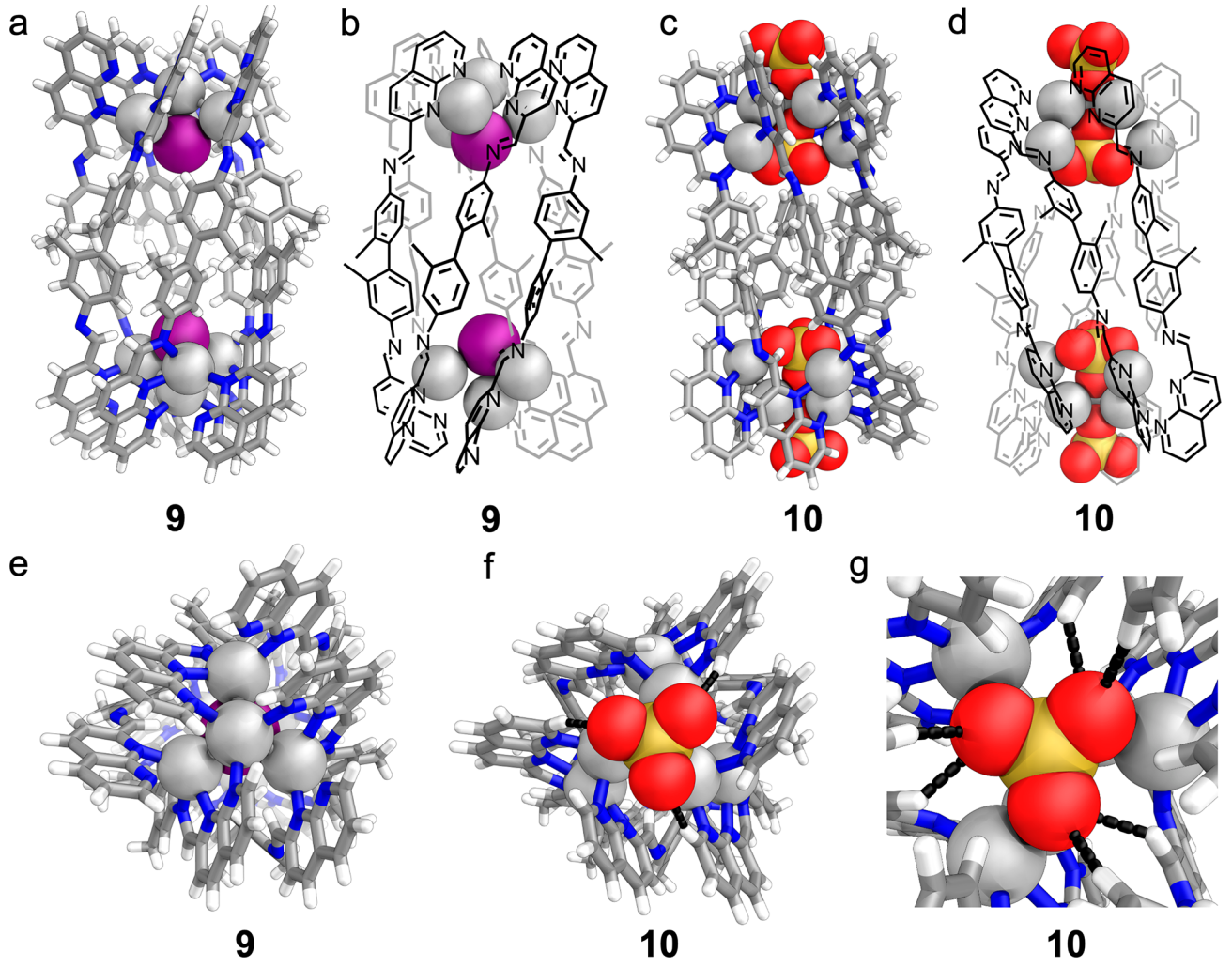

Figure 3. (a) X-ray crystal structure of **9**; (b) schematic view of **9**. (c) X-ray crystal structure of **10**; (d) schematic view of **10**. (e) End-on view of crystal structure of **9** showing cluster geometry. (f) End-on view of crystal structure of **10** showing the silver cluster and nonclassical hydrogen bonds to the exterior sulfate. (g) View from within the crystal structure of **10**, showing nonclassical hydrogen bonds to the internal sulfate.

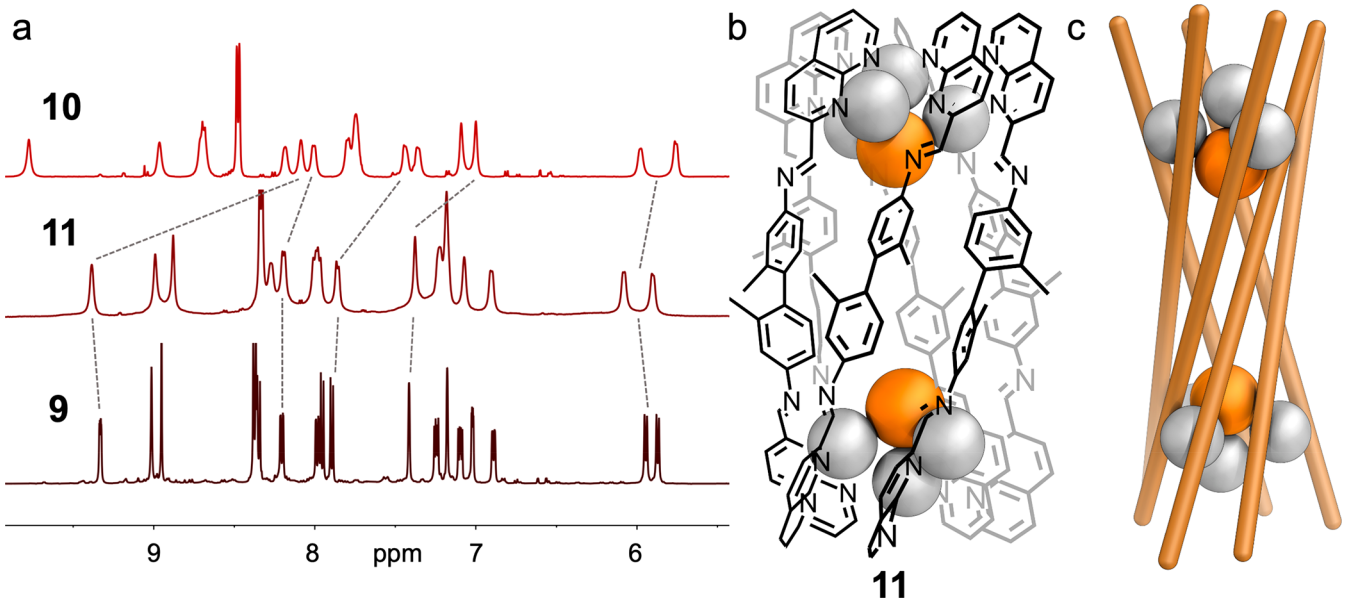

Figure 4. (a) Comparison of ^{1}H NMR spectra of **10** (top), **11** (middle), and **9** (bottom), showing the similarity between the spectra of **9** and **11**. Simplified (b) schematic and (c) cartoon views of six-stranded helicate **11**.

https://dx.doi.org/10.1021/jacs.0c11905
J. Am. Chem. Soc. 2021, 143, 664−670

The ability to use atomically precise clusters in place of mono- or dimetallic vertices in metal−organic cages has the potential to generate a vastly increased diversity of architectures, as we continue to uncover the principles underpinning silver−naphthyridine self-assembly. Future work will focus on exploring the photophysical properties of these novel clusters[66] and on expanding the range of architectures formed by the interplay of anion templation, ligand design, and coordinational flexibility to generate increased structural diversity.

■ ASSOCIATED CONTENT

Supporting Information

The Supporting Information is available free of charge at https://pubs.acs.org/doi/10.1021/jacs.0c11905.

Experimental procedure and details; MM3 models and calculated energies; mass spectrometry data; X-ray crystallography data (PDF)

X-ray data for **9** (CCDC 2024152) (CIF)

X-ray data for **10** (CCDC 2024153) (CIF)

■ AUTHOR INFORMATION

Corresponding Author

Jonathan R. Nitschke − *Department of Chemistry, University of Cambridge, Cambridge CB2 1EW, United Kingdom;* orcid.org/0000-0002-4060-5122; Email: jrn34@cam.ac.uk

Authors

Charlie T. McTernan − *Department of Chemistry, University of Cambridge, Cambridge CB2 1EW, United Kingdom;* orcid.org/0000-0003-1359-0663

Tanya K. Ronson − *Department of Chemistry, University of Cambridge, Cambridge CB2 1EW, United Kingdom;* orcid.org/0000-0002-6917-3685

Complete contact information is available at: https://pubs.acs.org/10.1021/jacs.0c11905

Notes

The authors declare no competing financial interest.

■ ACKNOWLEDGMENTS

This work was supported by the Engineering and Physical Sciences Research Council (EPSRC, EP/P027067/1) and the European Research Council (695009). We thank the University of Cambridge Mass Spectrometry Service Centre for high-resolution mass spectrometry and Diamond Light Source (UK) for synchrotron beamtime on I19 (CY21497). C.T.M. thanks the Leverhulme Trust and the Isaac Newton Trust, and Sidney Sussex College, Cambridge, for Fellowship support.

■ REFERENCES

(1) Danon, J. J.; Krüger, A.; Leigh, D. A.; Lemonnier, J.-F.; Stephens, A. J.; Vitorica-Yrezabal, I. J.; Woltering, S. L. Braiding a Molecular Knot with Eight Crossings. *Science* **2017**, *355*, 159−162.

(2) Wang, H.; et al. Assembling Pentatopic Terpyridine Ligands with Three Types of Coordination Moieties into a Giant Supramolecular Hexagonal Prism: Synthesis, Self-Assembly, Characterization, and Antimicrobial Study. *J. Am. Chem. Soc.* **2019**, *141*, 16108−16116.

(3) Fujita, D.; Ueda, Y.; Sato, S.; Yokoyama, H.; Mizuno, N.; Kumasaka, T.; Fujita, M. Self-Assembly of $M_{30}L_{60}$ Icosidodecahedron. *Chem* **2016**, *1*, 91−101.

(4) Niki, K.; Tsutsui, T.; Yamashina, M.; Akita, M.; Yoshizawa, M. Recognition and Stabilization of Unsaturated Fatty Acids by a Polyaromatic Receptor. *Angew. Chem., Int. Ed.* **2020**, *59*, 10489−10492.

(5) Howlader, P.; Mukherjee, P. S. Face and Edge Directed Self-Assembly of Pd_{12} Tetrahedral Nano-Cages and their Self-Sorting. *Chem. Sci.* **2016**, *7*, 5893−5899.

(6) Kaphan, D. M.; Levin, M. D.; Bergman, R. G.; Raymond, K. N.; Toste, F. D. A Supramolecular Microenvironment Strategy for Transition Metal Catalysis. *Science* **2015**, *350*, 1235−1238.

(7) Zhang, D.; Ronson, T. K.; Lavendomme, R.; Nitschke, J. R. Selective Separation of Polyaromatic Hydrocarbons by Phase Transfer of Coordination Cages. *J. Am. Chem. Soc.* **2019**, *141*, 18949−18953.

(8) Zhu, J.; Haynes, C. J. E.; Kieffer, M.; Greenfield, J. L.; Greenhalgh, R. D.; Nitschke, J. R.; Keyser, U. F. $Fe^{II}_4L_4$ Tetrahedron Binds to Nonpaired DNA Bases. *J. Am. Chem. Soc.* **2019**, *141*, 11358−11362.

(9) Hotze, A. C. G.; Kariuki, B. M.; Hannon, M. J. Dinuclear Double-Stranded Metallosupramolecular Ruthenium Complexes: Potential Anticancer Drugs. *Angew. Chem., Int. Ed.* **2006**, *45*, 4839−4842.

(10) Chen, B.; Holstein, J. J.; Horiuchi, S.; Hiller, W. G.; Clever, G. H. Pd(II) Coordination Sphere Engineering: Pyridine Cages, Quinoline Bowls, and Heteroleptic Pills Binding One or Two Fullerenes. *J. Am. Chem. Soc.* **2019**, *141*, 8907−8913.

(11) Rizzuto, F. J.; von Krbek, L. K. S.; Nitschke, J. R. Strategies for Binding Multiple Guests in Metal-Organic Cages. *Nat. Chem. Rev.* **2019**, *3*, 204−222.

(12) Takezawa, H.; Shitozawa, K.; Fujita, M. Enhanced Reactivity of Twisted Amides Inside a Molecular Cage. *Nat. Chem.* **2020**, *12*, 574−578.

(13) Chepelin, O.; et al. Luminescent, Enantiopure, Phenylatopyridine Iridium-Based Coordination Capsules. *J. Am. Chem. Soc.* **2012**, *134*, 19334−19337.

(14) Mosquera, J.; Ronson, T. K.; Nitschke, J. R. Subcomponent Flexibility Enables Conversion between D_4-Symmetric $Cd^{II}_4L_4$ Assemblies. *J. Am. Chem. Soc.* **2016**, *138*, 1812−1815.

(15) Cullen, W.; Misuraca, M. C.; Hunter, C. A.; Williams, N. H.; Ward, M. D. Highly efficient catalysis of the Kemp elimination in the cavity of a cubic coordination cage. *Nat. Chem.* **2016**, *8*, 231−236.

(16) Liu, Y.; Zhang, R.; He, C.; Dang, D. B.; Duan, C. Y. A Palladium(II) Triangle as Building Blocks of Microporous Molecular Materials: Structures and Catalytic Performance. *Chem. Commun.* **2010**, *46*, 746−748.

(17) Carpenter, J. P.; McTernan, C. T.; Ronson, T. K.; Nitschke, J. R. Anion Pairs Template a Trigonal Prism with Disilver Vertices. *J. Am. Chem. Soc.* **2019**, *141*, 11409−11413.

(18) Huang, S.; Lin, Y.; Hor, T. S. A.; Jin, J. Cp*Rh-based Heterometallic Metallarectangles: Size-Dependent Borromean Link Structures and Catalytic Acyl Transfer. *J. Am. Chem. Soc.* **2013**, *135*, 8125−8128.

(19) Yue, N. L. S.; Jennings, M. C.; Puddephatt, R. J. Disilver(I) Macrocycles: Variation of Cavity Size with Anion Binding. *Inorg. Chem.* **2005**, *44*, 1125−1131.

(20) Dong, Y.-B.; Geng, Y.; Ma, J.-P.; Huang, R.-Q. Organometallic Silver(I) Supramolecular Complexes Generated from Multidentate Furan-Containing Symmetric and Unsymmetric Fulvene Ligands and Silver(I) Salts. *Inorg. Chem.* **2005**, *44*, 1693−1703.

(21) Wang, Q.; Gonell, S.; Leenders, S. H. A. M.; Dürr, M.; Ivanović-Burmazović, I.; Reek, J. N. H. Self-Assembled Nanospheres with Multiple Endohedral Binding Sites Pre-Organize Catalysts and Substrates for Highly Efficient Reactions. *Nat. Chem.* **2016**, *8*, 225−230.

(22) Lisboa, L. S.; Findlay, J. A.; Wright, L. J.; Hartinger, C. G.; Crowley, J. D. A Reduced Symmetry Heterobimetallic $[PdPtL_4]^{4+}$ Cage: Assembly, Guest Binding and Stimulus-Induced Switching. *Angew. Chem., Int. Ed.* **2020**, *59*, 11101−11107.

(23) Ueda, Y.; Ito, H.; Fujita, D.; Fujita, M. Permeable Self-Assembled Molecular Containers for Catalyst Isolation Enabling

Two-Step Cascade Reactions. *J. Am. Chem. Soc.* **2017**, *139*, 6090−6093.
(24) Holloway, L. R.; Bogie, P. M.; Lyon, Y.; Ngai, C.; Miller, T. F.; Julian, R. R.; Hooley, R. J. Tandem Reactivity of a Self-Assembled Cage Catalyst with Endohedral Acid Groups. *J. Am. Chem. Soc.* **2018**, *140*, 8078−8081.
(25) Hua, B.; Shao, L.; Zhang, Z.; Liu, J.; Huang, F. Cooperative Silver Ion-Pair Recognition by Peralkylated Pillar[5]arenes. *J. Am. Chem. Soc.* **2019**, *141*, 15008−15012.
(26) Sawada, T.; Fujita, M. Folding and Assembly of Metal-Linked Peptidic Nanostructures. *Chem.* **2020**, *6*, 1861−1876.
(27) Sawada, T.; Inomata, Y.; Shimokawa, K.; Fujita, M. A Metal-Peptide Capsule by Multiple Ring Threading. *Nat. Commun.* **2019**, *10*, 5687.
(28) Inomata, Y.; Sawada, T.; Fujita, M. Metal-Peptide Torus Knots from Flexible Short Peptides. *Chem* **2020**, *6*, 294.
(29) Barendt, T. A.; Docker, A.; Marques, I.; Félix, V.; Beer, P. D. Selective Nitrate Recognition by a Halogen-Bonding Four-Station [3]Rotaxane Molecular Shuttle. *Angew. Chem., Int. Ed.* **2016**, *55*, 11069−11076.
(30) Langton, M. J.; Beer, P. D. Rotaxane and Catenane Host Structures for Sensing Charged Guest Species. *Acc. Chem. Res.* **2014**, *47*, 1935−1949.
(31) Kishi, N.; Akita, M.; Kamiya, M.; Hayashi, S.; Hsu, H.-F.; Yoshizawa, M. Facile Catch and Release of Fullerenes Using a Photoresponsive Molecular Tube. *J. Am. Chem. Soc.* **2013**, *135*, 12976−12979.
(32) Riddell, I. A.; Smulders, M. M. J.; Clegg, J. K.; Hristova, Y. R.; Breiner, B.; Thoburn, J. D.; Nitschke, J. R. Anion-induced Reconstitution of a Self-Assembly System to Express a Chloride-Binding $Co_{10}L_{15}$ Pentagonal Prism. *Nat. Chem.* **2012**, *4*, 751−756.
(33) Zhang, W.; Yang, D.; Zhao, J.; Hou, L.; Sessler, J. L.; Yang, Z.-J.; Wu, B. Controlling the Recognition and Reactivity of Alkyl Ammonium Guests Using an Anion Coordination-Based Tetrahedral Cage. *J. Am. Chem. Soc.* **2018**, *140*, 5248−5256.
(34) Custelcean, R. Anion Encapsulation and Dynamics in Self-Assembled Coordination Cages. *Chem. Soc. Rev.* **2014**, *43*, 1813−1824.
(35) Bowman-James, K. Alfred Werner Revisited: The Coordination Chemistry of Anions. *Acc. Chem. Res.* **2005**, *38*, 671−678.
(36) Custelcean, R.; Bonnesen, P. V.; Duncan, N. C.; Zhang, X.; Watson, L. A.; Van Berkel, G.; Parson, W. B.; Hay, B. P. Urea-Functionalized M_4L_6 Cage Receptors: Anion-Templated Self-Assembly and Selective Guest Exchange in Aqueous Solutions. *J. Am. Chem. Soc.* **2012**, *134*, 8525−8534.
(37) Liu, Y.; Zhao, W.; Chen, C.-H.; Flood, A. H. Chloride Capture Using a C-H Hydrogen-Bonding Cage. *Science* **2019**, *365*, 159−161.
(38) Liu, Y.; Sengupta, A.; Raghavachari, K.; Flood, A. M. Anion Binding in Solution: Beyond the Electrostatic Regime. *Chem* **2017**, *3*, 411−417.
(39) Zhao, W.; Qiao, B.; Tropp, J.; Pink, M.; Azoulay, J. D.; Flood, A. H. Linear Supramolecular Polymers Driven by Anion-Anion Dimerization of Difunctional Phosphonate Monomers Inside Cyanostar Macrocycles. *J. Am. Chem. Soc.* **2019**, *141*, 4980−4989.
(40) Wu, X.; Wang, P.; Turner, P.; Lewis, W.; Catal, O.; Thomas, D. S.; Gale, P. A. Tetraurea Macrocycles: Aggregation-Driven Binding of Chloride in Aqueous Solutions. *Chem.* **2019**, *5*, 1210−1222.
(41) Busschaert, N.; Caltagirone, C.; Van Rossom, W.; Gale, P. A. Applications of Supramolecular Anion Recognition. *Chem. Rev.* **2015**, *115*, 8038−8155.
(42) Chen, L.; Berry, S. N.; Wu, X.; Howe, E. N. W.; Gale, P. A. Advances in Anion Receptor Chemistry. *Chem.* **2020**, *6*, 61−141.
(43) Custelcean, R. Urea-Functionalized Crystalline Capsules for Recognition and Separation of Tetrahedral Oxoanions. *Chem. Commun.* **2013**, *49*, 2173−2182.
(44) Schäfer, S.; Gamer, M. T.; Lebedkin, S.; Weigend, F.; Kappes, M. M.; Roesky, P. W. Bis(6-methylene-2,2'-bipyridine)-phenylphosphine − A Flexible Ligand for the Construction of Trinuclear Coinage-Metal Complexes. *Chem. - Eur. J.* **2017**, *23*, 12198−12209.
(45) Luo, G.-G.; Guo, Q.-L.; Wang, Z.; Sun, C.-F.; Lin, J.-Q.; Sun, D. New Protective Ligands for Atomically Precise Silver Nanoclusters. *Dalton Trans.* **2020**, *49*, 5406−5415.
(46) Wang, X.; et al. Discrete Ag_6L_6 Coordination Nanotubular Structures Based on a T-Shaped Pyridyl Diphosphine. *Chem. Commun.* **2011**, *47*, 3849−3851.
(47) Zhang, Y.-W.; Bai, S.; Wang, Y.-Y.; Han, Y.-F. A Strategy for the Construction of Triply Interlocked Organometallic Cages by Rational Design of Poly-NHC Precursors. *J. Am. Chem. Soc.* **2020**, *142*, 13614−13621.
(48) Jin, G.-X.; Zhu, G.-Y.; Sun, Y.-Y.; Shi, Q.-X.; Liang, L.-P.; Wang, H.-Y.; Wu, Z.-W.; Ma, J.-P. $[Ag\text{-}Ag]^{2+}$ Unit-Encapsulated Trimetallic Cages: One-Pot Syntheses and Modulation of Argentophilic Interactions by the Uncoordinated Substituents. *Inorg. Chem.* **2019**, *58*, 2916−2920.
(49) Schmidbaur, H.; Schier, A. Argentophilic Interactions. *Angew. Chem., Int. Ed.* **2015**, *54*, 746−784.
(50) Zhang, Q.-Y.; He, X.; Zhao, L. Macrocycle-Assisted Synthesis of Non-Stoichimetric Silver(I) Halide Electrocatalysts for Efficient Chlorine Evolution Reaction. *Chem. Sci.* **2017**, *8*, 5662−5668.
(51) Zhang, S.; Zhao, L. Macrocycle-Encircled Polynuclear Metal Clusters: Controllable Synthesis, Reactivity Studies, and Applications. *Acc. Chem. Res.* **2018**, *51*, 2535−2545.
(52) Desnoyer, A. N.; Nicolay, A.; Rios, P.; Ziegler, M. S.; Tilley, T. D. Bimetallics in a Nutshell: Complexes Supported by Chelating Naphthyridine-Based Ligands. *Acc. Chem. Res.* **2020**, *53*, 1944−1956.
(53) Jansze, S. M.; et al. Ligand Aspect Ratio as a Decisive Factor for the Self-Assembly of Coordination Cages. *J. Am. Chem. Soc.* **2016**, *138*, 2046−2054.
(54) Giuseppone, N.; Schmitt, J.-L.; Allouche, L.; Lehn, J.-M. DOSY NMR Experiments as a Tool for the Analysis of Constitutional and Motional Dynamic Processes: Implementation for the Driven Evolution of Dynamic Combinatorial Libraries of Helical Strands. *Angew. Chem., Int. Ed.* **2008**, *47*, 2235−2239.
(55) Zhang, Z.; et al. Intra- and Intermolecular Self-Assembly of a 20-nm-Wide Supramolecular Hexagonal Grid. *Nat. Chem.* **2020**, *12*, 468−474.
(56) Although the coordinative flexibility shown by the napthyridine−silver system limits the degree of certainty of these modeling results, the large difference in energy between the tetrahedral architecture and alternate structures lends credence to the assignment of the Ag_8L_6 structure as a tetrahedron.
(57) For example: von Krbek, L. K. S.; Roberts, D. A.; Pilgrim, B. S.; Schalley, C. A.; Nitschke, J. R. Multivalent Crown-ether Receptors Enable Allosteric Regulation of Anion Exchange in an Fe_4L_6 Tetrahedron. *Angew. Chem., Int. Ed.* **2018**, *57*, 14121−14124.
(58) Clegg, J. K.; Cremers, J.; Hogben, A. J.; Breiner, B.; Smulders, M. M. J.; Thoburn, J. D.; Nitschke, J. R. A Stimuli Responsive System of Self-Assembled Anion-Binding $Fe_4L_6^{8+}$ Cages. *Chem. Sci.* **2013**, *4*, 68−76.
(59) Fernández-Galán, R.; Manzano, B. R.; Otero, A.; Lanfranchi, M.; Pellinghelli, M. A. ^{19}F and ^{31}P NMR Evidence for Silver Hexafluorophosphate Hydrolysis in Solution. New Palladium Difluorophosphate Complexes and X-ray Structure Determination of $[Pd(\eta^3\text{-}2\text{-}Me\text{-}C_3H_4)(PO_2F_2)(PCy_3)]$. *Inorg. Chem.* **1994**, *33*, 2309−2312.
(60) Salomon, M. Solubilities of the Silver Halides in Benzonitrile and Trichloroacetonitrile Mixtures with Propylene Carbonate. *Can. J. Chem.* **1976**, *54*, 1487−1492.
(61) Mass spectrometry of these silver complexes is challenging, presumably due to the dynamic nature of the naphthyridine−silver interactions. We see extensive fragmentation of all complexes under even mild conditions. By tuning ionization conditions and through choice of counterion, we were able to gather data on these architectures in both LRMS and HRMS. We found that using hexafluorophosphate as the counterion was particularly effective for obtaining good quality mass spectra.

https://dx.doi.org/10.1021/jacs.0c11905
J. Am. Chem. Soc. 2021, 143, 664−670

(62) Lehn, J.-M. Toward Complex matter: Supramolecular Chemistry and Self-Organization. *Proc. Natl. Acad. Sci. U. S. A.* **2002**, *99*, 4763−4768.
(63) Toyota, S.; Woods, C. R.; Benaglia, M.; Haldimann, R.; Wärnmark, K.; Hardcastle, K.; Siegel, J. S. Tetranuclear Copper(I)-Biphenanthroline Gridwork: Violation of the Principle of Maximal Donor Coordination Caused by Intercalation and CH-to-N Forces. *Angew. Chem., Int. Ed.* **2001**, *40*, 751−754.
(64) A minor isomer was also resolved in the crystallographic data, whereby an exterior sulfate coordinates via three oxygen atoms instead. Please see SI Section 12 for further details.
(65) Fatila, E. M.; Twum, E. B.; Sengupta, A.; Pink, M.; Karty, J. A.; Raghavachari, K.; Flood, A. H. Anion Stabilize Each Other Inside Macrocyclic Hosts. *Angew. Chem., Int. Ed.* **2016**, *55*, 14057−14062.
(66) These silver−naphthyridine systems proved to be extremely stable to light, which was unexpected. Samples could be left exposed to ambient light for 2−3 months with no sign of decomposition by NMR, or precipitation.

https://dx.doi.org/10.1021/jacs.0c11905
J. Am. Chem. Soc. 2021, 143, 664−670